MODELLING THE SLOW CRACK GROWTH DUE TO INTERNAL HYDROGEN IN METALS

WEIJIE WU [1], *YANFEI WANG* [2], *LIMIN SHEN* [2], *JIANMING GONG* [1]

[1] *School of Mechanical and Power Engineering, Nanjing Tech University, Nanjing, China;*

[2] *School of Chemical Engineering and Technology, China University of Mining and Technology, Xuzhou, China*

Hydrogen-induced slow crack growth generally exhibits three distinct stages of crack growth kinetics, and stages I and II are hydrogen diffusion-controlled. A model describing the crack growth kinetics of stages I and II due to internal hydrogen is proposed, based on the linear-elastic fracture mechanics, stress-induced hydrogen diffusion theory and hydrogen-enhanced decohesion mechanism for hydrogen-induced cracking. The model predicts the crack growth rate da/dt of both stages I and II as a function of the stress intensity factor K_I and initial hydrogen concentration level. Some experimental data reported in literature are used to validate the model and a good agreement is obtained.

Keywords: *hydrogen-induced cracking, hydrogen diffusion, crack growth, hydrogen embrittlement.*

Hydrogen-induced slow crack growth is a well-known phenomenon in metals science [1–2]. The kinetics of crack growth has been widely investigated by means of both experimental testing and theoretical modelling. For instance, previously, Gerberich et al. [3] investigated the crack growth kinetics of AISI 4340 high-strength steel after cathodical hydrogen-charging, and provided a short-time diffusion correlation for the kinetics. Andreikiv et al. [4] presented an overview regarding the theoretical aspects of hydrogen-induced crack growth kinetics and pointed out that further theoretical investigations of the kinetics should be directed toward the development of analytical models taking into account the influence of various supply mechanisms of hydrogen to the potential crack initiation sites. Moody et al. [5] tested the slow crack growth induced by internal hydrogen in iron-based alloy IN903. Singh and Altstetter [6] studied the effect of various levels of internal hydrogen concentration on the crack growth in 301; 304 and 310S stainless steels. Andreikiv and Rudavs'kyi [7] obtained an approximate solution of hydrogen diffusion problem in the vicinity of the crack tip and established the dependence of the crack growth rate on the crack tip opening displacement. In addition, Gangloff et al. [8] studied the cracking in modern ultra-high-strength Monel K-500 steel induced by internal hydrogen through combined experimental testing and theoretical modelling. Hembara et al. [9] proposed an experimental-theoretical approach to predict the crack propagation and to determine the residual durability of vessels in gaseous hydrogen.

In the above studies, typical three distinct stages of crack growth kinetics describing the crack growth rate da/dt as a function of the stress intensity factor (SIF) K_I (Fig. 1) are reported. The rate of stage I, which is the stage nearest to the K_{Ith} (the threshold SIF for the hydrogen-induced slow crack growth below which no crack growth will occur even in the presence of hydrogen), is strongly dependent on the applied K_I, while the rate of stage II is less affected by K_I. In some cases the crack growth

Corresponding author: YANFEI WANG, e-mail: wyf_hg@outlook.com

rate of stage II is even found to be virtually independent of K_I [4–6]. As K_I is further increased to be close to the critical SIF K_{IC} of metal, the da/dt increases largely and is again strongly dependent on K_I (stage III). The stages I and II have been established as the hydrogen diffusion-controlled process [4–7]. It is believed that when the hydrogen concentration at the prospective crack initiation site ahead of the crack tip is accumulated to exceed a critical value through stress-induced hydrogen diffusion [10], a new microcrack will initiate at this prospective site and then it will coalesce with the original crack tip, resulting in the increment of the crack length i.e. crack growth. By repeating this process the crack grows longer and longer, eventually causing the complete fracture of metals.

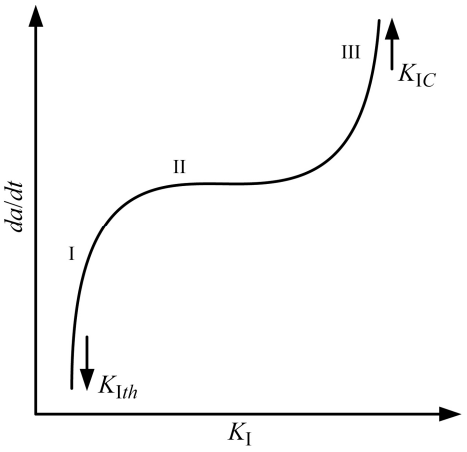

Fig. 1. Typical three distinct stages of crack growth kinetics due to hydrogen in metals.

A very simple model describing the crack growth kinetics i.e. $da/dt \sim K_I$ of stages I and II for metals containing internal hydrogen is derived based on the linear-elastic fracture mechanics, stress-induced hydrogen diffusion theory and hydrogen-enhanced decohesion mechanism of hydrogen-induced cracking. Experimental data in [3, 5–6] were used to verify the model.

Procedure of the model. In general, the driven force for diffusion of hydrogen in metals is the gradient of chemical potential μ, which is a function of hydrogen concentration C, temperature T and hydrostatic stress σ_h. For the region ahead of the loaded crack tip, due to the presence of very high local stress, the μ is mainly stress-dependent, thus

$$\mu = \mu_0 - \Omega\sigma_h, \tag{1}$$

where μ_0 is a fixed value; σ_h is the hydrostatic stress; and Ω is the partial volume of an interstitial hydrogen, 3.818 Å^3 for most steels. According to the linear-elastic fracture mechanics, the σ_h field ahead of the crack tip for plain strain conditions under Mode-I loading can be expressed as

$$\sigma_h = \frac{\sigma_{xx} + \sigma_{yy} + \sigma_{zz}}{3} = \frac{2(1+\nu)}{3} \cdot \frac{K_I}{\sqrt{2\pi r}} \cos\frac{\theta}{2}, \tag{2}$$

where v is the Poisson's ratio. Under the gradient μ, the force acting on a hydrogen atom is

$$\vec{f} = -\nabla\mu. \tag{3}$$

The velocity of the hydrogen atom is thus

$$\vec{v} = \frac{D\vec{f}}{kT} = -\frac{D}{kT}(\nabla\mu), \tag{4}$$

where D is the hydrogen diffusivity; k is the Boltzmann constant. The component of velocity towards the crack tip $r \approx 0$ is

$$v_r = -\frac{D}{kT}(\nabla\mu)_r = \frac{(1+\nu)}{3\sqrt{2\pi}} \cdot \frac{D\Omega}{kT} \cdot \frac{K_I}{r^{3/2}} \cos\frac{\theta}{2}. \tag{5}$$

Thus, after time t, all the hydrogen atoms within radius $r = R$ can arrive at the immediate crack tip $r \approx 0$ [11]. Then R is

$$R = \left[\frac{5(1+\nu)}{12\sqrt{2\pi}} \cdot \frac{D\Omega K_{\mathrm{I}}}{kT} \cdot t \cdot \cos\frac{\theta}{2} \right]^{2/5} . \tag{6}$$

The area of the region with $r = R$ is

$$A_R = \int_{-\pi}^{\pi} \frac{R^2}{2} d\theta = \beta\left(\frac{1}{2}, \frac{9}{10}\right) \left[\frac{5(1+\nu)}{12\sqrt{2\pi}} \cdot \frac{D\Omega K_{\mathrm{I}}}{kT} \cdot t \right]^{4/5} , \tag{7}$$

where β is the Beta function. Assuming that all the hydrogen atoms arriving at $r \approx 0$ finally concentrate in the small zone ahead of the crack tip, which is generally known as the fracture process zone (FPZ), the hydrogen concentration c_{FPZ} in this FPZ is thus

$$c_{\mathrm{FPZ}} = \frac{c_0 A_R}{A_{\mathrm{FPZ}}} , \tag{8}$$

where c_0 is the initial uniform concentration, A_{FPZ} is the FPZ area. When the c_{FPZ} reaches the critical value c_{cr} for crack initiation, a new microcrack initiates in the FPZ, and then it coalesces with the original crack, resulting in the crack length increment. For the increment time, one can get

$$c_{cr} = \frac{c_0}{A_{\mathrm{FPZ}}} \cdot \beta\left(\frac{1}{2}, \frac{9}{10}\right) \left[\frac{5(1+\nu)}{12\sqrt{2\pi}} \cdot \frac{D\Omega K_{\mathrm{I}}}{kT} \cdot \Delta t \right]^{4/5} , \tag{9}$$

where Δt is the time interval between two crack increments. Thus, the crack growth rate can be approximately determined as

$$\frac{da}{dt} \approx \frac{\Delta L}{\Delta t} = \frac{5(1+\nu)}{12\sqrt{2\pi}} \cdot \frac{D\Omega}{kT} \cdot \Delta L \cdot K_{\mathrm{I}} \cdot \left[\frac{c_{cr}}{c_0} \frac{A_{\mathrm{FPZ}}}{\beta(1/2,\, 9/10)} \right]^{-5/4} , \tag{10}$$

where ΔL is the so-called characteristic fracture distance, i.e. the distance between the crack initiation site and the original crack tip. Eq. (10) indicates that the hydrogen-induced slow crack growth rate increases linearly with increasing K_{I}, being in agreement with the experimental results reported in [3] for lower K_{I}. However, the experimental data have demonstrated that there is a threshold value for the K_{I}, i.e. the threshold SIF for hydrogen-induced crack growth, $K_{\mathrm{I}th}$, below which no crack growth will be observed even in the presence of hydrogen (Fig. 1). Thus, it seems that only the part exceeding the $K_{\mathrm{I}th}$, i.e. $(K_{\mathrm{I}}–K_{\mathrm{I}th})$, drives the process. Thus, Eq. (10) should be modified as

$$\frac{da}{dt} \approx \frac{5(1+\nu)}{12\sqrt{2\pi}} \cdot \frac{D\Omega}{kT} \cdot \Delta L \cdot (K_{\mathrm{I}} - K_{\mathrm{I}th}) \cdot \left[\frac{c_{cr}}{c_0} \frac{A_{\mathrm{FPZ}}}{\beta(1/2, 9/10)} \right]^{-5/4} . \tag{11}$$

Eq. (11) is the proposed simple model for the hydrogen-induced slow crack growth kinetics in metals, which describes the dependence of crack growth rate on the SIF K_{I} and initial hydrogen concentration level c_0.

Validation with experiment data. Experimental data on $da/dt \sim K_{\mathrm{I}}$ for the iron-based IN903 alloy, 304 stainless steel and 4340 high-strength steel, as reproduced in Fig. 2 from the studies of Moody et al. [5], Singh and Altstetter [6] and Gerberich et al. [3], respectively, are used to validate the model, i.e. Eq. (11).

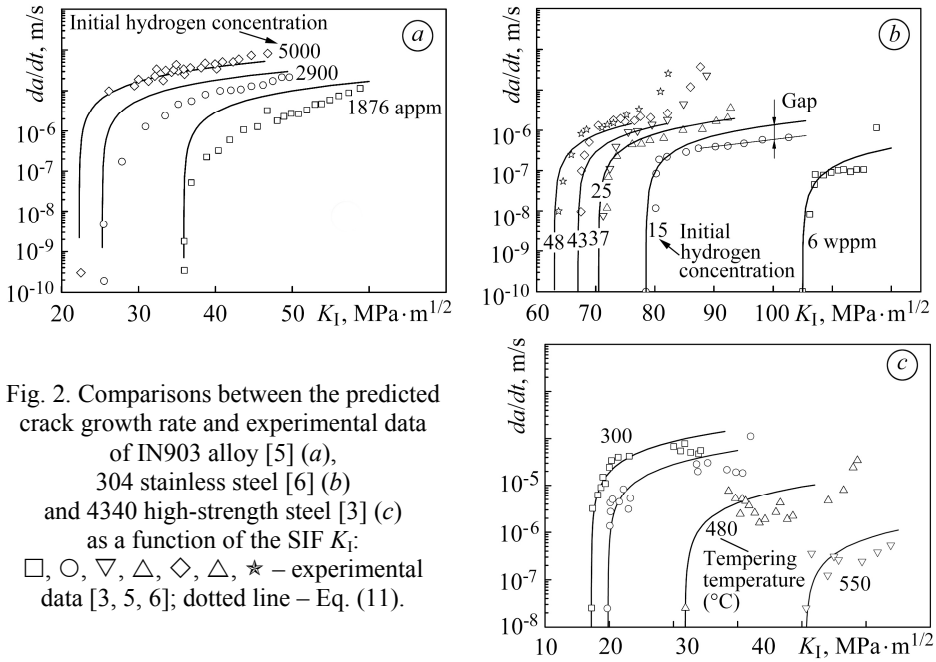

Fig. 2. Comparisons between the predicted crack growth rate and experimental data of IN903 alloy [5] (*a*), 304 stainless steel [6] (*b*) and 4340 high-strength steel [3] (*c*) as a function of the SIF K_I: □, ○, ▽, △, ◇, △, ✯ – experimental data [3, 5, 6]; dotted line – Eq. (11).

To apply Eq. (11) the parameters ΔL, A_{FPZ}, and c_{cr} of the three metals are required. The matrix carbide spacing was established as the characteristic fracture distance for the IN903 alloy because slip band fracture was observed for this alloy after hydrogenation [5]. Thus, the ΔL of the IN903 alloy in [5] was taken as the average matrix carbide spacing of the alloy, i.e. 19.5 μm, as suggested by Moody et al. [5]. The characteristic fracture distance of the 304 steel in [6] is unknown. However, a fraction of intergranular fracture was observed in the 301 steel which was investigated together with the 304 steel by Altstetter et al. in [6]. Average grain size can be taken as the fracture distance for intergranular fracture [3]. Since both 304 and 301 steels are unstable Cr–Ni stainless steels, the ΔL for the 304 steel are approximately taken as the grain size of the steel, i.e. about 100 μm, as demonstrated by the SEM fracture surface pictures [6]. The characteristic fracture distance of the 4340 high-strength steel is also taken as the grain size of the steel, i.e. 20 μm, as suggested by Gerberich et al. [3]. It is reasonable to assume that the FPZ is a circular zone and the crack initiation site is located in the centre of the FPZ, so, $L_{FPZ} = 2\Delta L$ with L_{FPZ} is the length of FPZ along crack plane, thus the A_{FPZ} is

$$A_{FPZ} = \pi(\Delta L)^2 . \tag{12}$$

The authors [5, 6] focused on the effect of initial hydrogen concentration level on the crack growth rate. The K_{Ith} values at various initial hydrogen concentration levels c_0 were given for the IN903 alloy and 304 steel, respectively. The authors [3] focused on the effect of tempering temperature while keeping the initial hydrogen concentration level constant. The K_{Ith} values were given for the 3040 steel after tempering at various temperatures. It is clear that under the K_{Ith} action, the maximum hydrogen concentration at the crack tip through the stress-assisted diffusion can be taken as the critical hydrogen concentration for crack initiation [10]. Hence the critical hydrogen concentration is expressed as

$$c_{cr} = c_{max} = c_0 \exp\left[\frac{2(1+\nu)K_{IH}}{3\sqrt{2\pi \cdot \Delta L}}\frac{\Omega}{kT}\right]. \tag{13}$$

Based on the above mentioned, the parameters ΔL, A_{FPZ}, and c_{cr} for the IN903 alloy, 304 and 4340 steels are obtained (Tables 1–3). The other parameters used are also given in Tables 1–3. The c_0 and K_{Ith} data were reproduced from [3, 5–6]. It should be noted that the hydrogen diffusivity in the 304 steel is taken as that in the α′ martensite phase, as suggested by Altstetter et al. in [6], because the 304 steel is unstable. Under the action of K_I, the austenite phase ahead of the crack tip should be transformed into the α′ martensite phase, consequently drastically increasing the apparent hydrogen diffusivity in the 304 steel [6]. It is known that hydrogen diffusivity in the α′ martensite phase is about five orders of magnitude higher than that in the full austenite phase [6]. In addition, for the 4340 steel it is known that a higher tempering temperature can increase the number of effective traps such as precipitates and thus decrease the diffusivity. The reported diffusivity for the high-strength steels ranges from $2\cdot10^{-12}$ (for the steel with a large number of hydrogen traps) to $2\cdot10^{-8}$ m^2/s (for the steel with few traps) [13]. The diffusivity of hydrogen in the 4340 steel tempered at 300°C is taken as $2\cdot10^{-8}$ m^2/s, as it gives the best fit to the experimental data. For the steel tempered at other temperatures the diffusivity is assumed to decrease proportionally with increasing tempering temperature (Table 3). Note that in Tables 1–3 it is shown that the critical hydrogen concentration can be from several times to thirty times higher than the initial average hydrogen concentration. This is in line with the results in literature. For instance, the experimental results of Yu et al. [14] show that the accumulation coefficients of hydrogen (a ratio of maximum hydrogen concentration to initial hydrogen concentration) at the grain boundaries, various inclusions, and near the loaded notch tip of steel can reach 2.2 to 11, 8 to 20, and 2.5 to 4.5, respectively. Balyts'kyi et al. and Dmytrakh et al. have demonstrated similar results by experimental measurements or combined measurements and numerical simulations [15–17].

Table 1. The parameters used for the IN903 iron-based alloy

Material	D, m^2/s	d, μm	c_0, appm (atom fraction)	$K_{I\,H}$, $MPa\sqrt{m}$	c_{cr}, appm
IN903	$9.6\cdot10^{-9}$ [12]	19.5	1876	35.9	20320
			2900	26.3	16612
			5000	22.3	21963

Table 2. The parameters used for the 304 stainless steel

Material	D, m^2/s	d, μm	c_0, wppm (weight fraction)	$K_{I\,H}$, $MPa\sqrt{m}$	c_{cr}, wppm
304	$9.3\cdot10^{-9}$ [6]	100	6	105	130
			15	78.5	150
			25	70.5	197
			37	70.5	292
			43	67	306
			48	63	304

The da/dt for the three metals is predicted by Eq. (11) (Fig. 2). It is shown that the predicted results are in good agreement with experimental data, indicating that the proposed simple model i.e. Eq. (11) has a potential to predict the hydrogen-induced slow

crack growth rate under the action of internal hydrogen. Particularly, the model accurately predicts the transitions from stage I to stage II for all $da/dt \sim K_I$ curves.

Table 3. The parameters used for the 4340 high-strength steel

Material	Tempering temperature, °C	D, m^2/s	d, μm	c_0, appm (atom fraction)	K_{IH}, $MPa\sqrt{m}$	c_{cr}, appm
4340	300	$2 \cdot 10^{-8}$ [13]	20	2.6	17.2	8.0
	400	$1 \cdot 10^{-8}$			19.8	9.5
	480	$5 \cdot 10^{-9}$			31.8	20.9
	550	$2.5 \cdot 10^{-9}$			50.6	71.6

Taking the IN903 alloy as an example, Fig. 3 shows the calculated shape and size of the region of $r = R$ at (c_0 = 1876 appm, $K_I = 36.0$ $MPa\sqrt{m}$ and (c_0 = 5000 appm, $K_I = 22.5$ $MPa\sqrt{m}$), respectively. All hydrogen atoms in the region R enter into the FPZ by stress-assisted diffusion and then cause crack initiation and growth. With increasing c_0, the size of the region decreases, because there is no much difference between the critical hydrogen concentrations of the two cases.

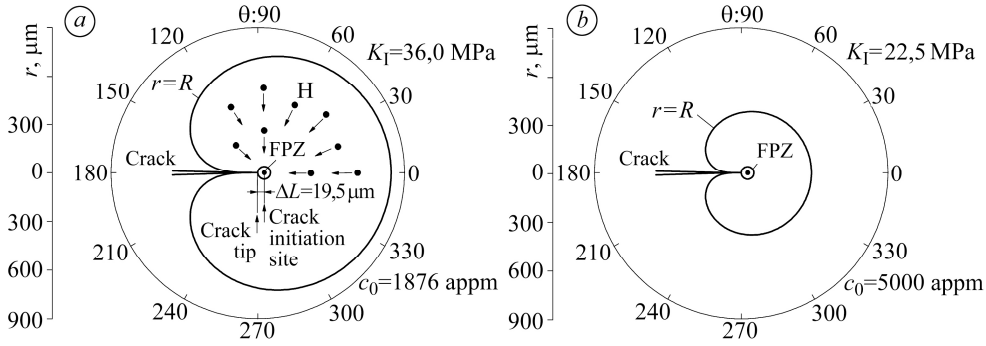

Fig. 3. The calculated shape and size of the region of $r = R$ under (c_0 = 1876 appm, $K_I = 36.0$ $MPa\sqrt{m}$) (*a*) and (c_0 = 5000 appm, $K_I = 22.5$ $MPa\sqrt{m}$) (*b*) for the IN903 iron-based alloy.

It should be noted that the plastic deformation ahead of the crack tip is not considered in Eq. (11). The presence of plastic deformation may reduce the stress at the immediate crack tip, and then reduce the average velocity of hydrogen atoms approaching to the crack tip, as a result, the time interval between two crack increments should increase. Thus, although some assumptions are introduced into the model, since the plastic deformation is not considered, Eq. (11) provides a conservative estimation of the hydrogen-induced slow crack growth rate. This can be confirmed by Fig. 2 as it demonstrates that a higher K_I brings a bigger gap between the predicted rate and experimental rate. A conservative estimation of the crack growth rate is acceptable for the security and from a life design perspective.

CONCLUSION

A very simple model to predict the crack growth rate of stages I and II due to internal hydrogen in metals based on the linear-elastic fracture mechanics, stress-induced hydrogen diffusion theory and hydrogen-enhanced decohesion mechanism for hydrogen-induced cracking is provided. The model describes the crack growth rate

da/*dt* of stages I and II as a function of the SIF K_I and initial hydrogen concentration level c_0. The predicted results match very well with the experimental data in literature. The plastic deformation ahead of the crack tip is not considered in the model, thus the estimation of the crack growth rate based on the model is slightly conservative for higher K_I.

РЕЗЮМЕ. Повільний ріст спричинених воднем тріщин, як правило, має три різні стадії. Ріст тріщини на стадіях I і II визначає дифузія водню. Запропоновано модель, яка описує кінетику росту водневої тріщини на першій і другій стадіях, викликаної механічними напруженнями і посиленого воднем механізму декогезії під час водневого розтріскування, на основі лінійної механіки руйнування, теорії дифузії водню. Модель дає змогу прогнозувати швидкість росту тріщини *da*/*dt* залежно від коефіцієнта інтенсивності напружень K_I і початкової концентрації водню. Для перевірки теоретичної моделі використовували подані в літературі експериментальні результати і отримали їх задовільну збіжність.

РЕЗЮМЕ. Медленный рост трещин, вызванных водородом, как правило, имеет три различных стадии. Рост трещины на стадиях I и II определяет диффузия водорода. Предложено модель, описывающую кинетику роста водородной трещины на первой и второй стадиях, вызванной механическим напряжением и усиленного водородом механизма декогезии при водородном растрескивании, на основе линейной механики разрушения, теории диффузии водорода. Модель позволяет прогнозировать скорость роста трещины *da*/*dt* в зависимости от коэффициента интенсивности напряжений K_I и начальной концентрации водорода. Для проверки теоретической модели использовали представленные в литературе экспериментальные результаты и получили их удовлетворительное совпадение.

Acknowledgements. This work is supported by the National Natural Science Foundation of China (51505477) and the Fundamental Research Funds for the Central Universities of China (2015QNA20).

1. *Панасюк В. В., Андрейкив А. Е., Харин В. С.* Модель роста трещин в деформированных металлах при воздействии водорода // Физ.-хим. механика материалов. – 1987. – **23**, № 2. – С. 3 – 16.

   (*Panasyuk V. V., Andreikiv A. E., and Kharin V. S.* A model of crack growth in deformed metals under the action of hydrogen // Soviet Materials Science. – 1987. – **23**, № 2. – P. 111–124.)

2. *Вплив* водню на опірність руйнуванню листової сталі 65Г / Я. Л. Іваницький, С. Т. Штаюра, Ю. В. Мольков, Т. М. Ленковський // Фіз.-хім. механіка матеріалів. – 2011. – **47**, № 4. – С. 36–40.

   (*Influence* of hydrogen on the fracture resistance of 65G sheet steel / Ya. L. Ivanyts'kyi, S. T. Shtayura, Yu. V. Mol'kov, and T. M. Lenkovs'kyi // Materials Science. – 2012. – **47**, № 4. – P. 457–461.)

3. *Gerberich W. W., Chen Y. T., and John C. S. T.* A short-time diffusion correlation for hydrogen-induced crack growth kinetics // Metall. Transact. A. – 1975. – **6.** – P. 1485–1498.

4. *Андрейкив А.* Е., Панасюк В. В., Харин В. С. Теоретические аспекты кинетики водородного охрупчивания металлов // Физ.-хим. механика материалов. – 1978. – **14**, № 3. – С. 3–23.

   (*Andreikiv A. E., Panasyuk V. V., and Kharin V. S.* Theoretical aspects of the kinetics of hydrogen embrittlement of metals // Materials Science. – 1978. – **14**, № 3. – P. 227–244.)

5. *Moody N. R., Robinson S. L., and Perra M. W.* Internal hydrogen effects on thresholds for crack growth in the iron-based super alloy IN903 // Eng. Fract. Mech. – 1991. – **39**, № 6. – P. 941–954.

6. *Singh S. and Altstetter C. J.* Effects of hydrogen concentration on slow crack growth in stainless steels // Metall. Transact. A. – 1982. – **13**, № 10. – P. 1799–1808.

7. *Андрейків О. Є., Руданський Д. В.* Розрахунок ресурсу елемента трубопроводу під впливом водневовмісного середовища // Фіз.-хім. механіка матеріалів. – 1999. – **35**, № 4. – С. 43–48.

(*Andreikiv O. E. and Rudavs'kyi D. V.* Prediction of the service life of pipeline elements subjected to the action of hydrogen-containing media // Materials Science. – 1999. – **35**, № 4. – P. 491–498.)

8. *Measurement* and modeling of hydrogen environment-assisted cracking in Monel K-500 / R. P. Gangloff, H. M. Ha, J. T. Burns, and J. R. Scully // Metall. Mater. Trans. A. – 2014. – **45A**, № 9. – P. 3814–3834.
9. *Toribio J., and Kharin V.* Effect of residual stress-strain profiles on hydrogen-induced fracture of prestressing steel wires // Фіз.-хім. механіка матеріалів. – 2006. – **42**, № 2. – С. 105–112.

   (*Toribio J., and Kharin V.* Effect of residual stress-strain profiles on hydrogen-induced fracture of prestressing steel wires // Materials Science. – 2006. – **42**, № 2. – P. 263–271.)
10. *Wang Y. F., Gong J. M., and Jiang W. C.* A quantitative description on fracture toughness of steels in hydrogen gas // Int. J. Hydrogen Energy. – 2013. – **38**, № 28. – P. 12503–12508.
11. *Song J. and Curtin W. A.* Atomic mechanism and prediction of hydrogen embrittlement in iron // Nature Materials. – 2013. – **12**. – P. 145–151.
12. *Robertson W. M.* Hydrogen permeation and diffusion in inconel 718 and incoloy 903 // Metall. Transact. A. – 1977. – **8**, № 11. – P. 1709–1712.
13. *Oriani R. A.* The diffusion and trapping of hydrogen in steel // Acta Metall. – 1970. – **8**. – P. 147–157.
14. *Hydrogen* accumulation and hydrogen-induced cracking of API C90 tubular steel / G. H. Yu, Y. H. Cheng, L. Chen, L. J. Qiao, Y. B. Wang, and W. Y. Chu // Corrosion. – 1997. – **53**, № 10. – P. 762–769.
15. *Вплив* водню на тріщиностійкість сталі 10Х15Н27Т3В2МР / О. І. Балицький, Л. М. Іваськевич, В. М. Мочульський, О. М. Голіян // Фіз.-хім. механіка матеріалів. – 2009. – **45**, № 2. – С. 102–110.

   (*Influence* of hydrogen on the crack resistance of 10Kh15N27T3V2MR steel // O. I. Balyts'kyi, L. M. Ivas'kevych, V. M. Mochul's'kyi, and O. M. Holiyan // Materials Science. – 2009. – **45**, № 2. – P. 258–267.
16. *Іваськевич Л. М., Галицький О. І., Мочульський В. М.* Вплив водню на статичну тріщиностійкість жароміцних сталей // Фіз.-хім. механіка матеріалів. – 2012. – **48**, № 3. – С. 78–86.

   (*Ivas'kevych L. M., Balyts'kyi O. I., and Mochul's'kyi V. M.* Influence of hydrogen on the static crack resistance of refractory steels // Materials Science. – 2012. – **48**, № 3. – P. 345–353.)
17. *Relationship* between fatigue crack growth behaviour and local hydrogen concentration near crack tip in pipeline steel / I. M. Dmytrakh, O. D. Smiyan, A. M. Syrotyuk, and O. L. Bilyy // Int. J. Fatig. – 2013. – **50**. – P. 26–32.

Received 05.08.2016